

# Microstructural Maturations of the Anterior Cruciate Ligament and the Medial Collateral Ligament During the Postnatal Development in Murine

Haruki Tsunogae<sup>1</sup>, Yuna Usami<sup>2</sup>, Riku Saito<sup>2</sup>, Tetsuya Yano<sup>2</sup>, Takanori Kokubun<sup>1,2</sup>

<sup>1</sup> Department of Physical Therapy, School of Health and Social Services, Saitama Prefectural University, Saitama, Japan

<sup>2</sup> Graduate School of Health, Medicine, and Welfare, Saitama Prefecture University, Saitama, Japan,

Email: 2513023f@spu.ac.jp

**Disclosures:** All authors have no disclosures

**INTRODUCTION:** The anterior cruciate ligament (ACL) performs an essential role in controlling and stabilizing knee motion. Although the ACL is the most commonly injured knee ligament, multiple studies have shown that ACLs have limited self-healing capacity. On the other hand, MCL is known to exhibit superior intrinsic healing capacity. Since synovial fluid surrounds the injured ACL, this unique environment influences the low healing potential of the ACL. In contrast, the medial collateral ligament (MCL) and all other extraarticular ligaments heal well spontaneously. It has been reported that a completely ruptured ACL can heal spontaneously by controlling anterior tibial translation<sup>1</sup>. However, the healed ACL showed obviously low mechanical properties. During the healing process, some biological courses resemble the developmental process. In particular, fibril formation is a key event in both development and healing, enabling the acquisition of substantial mechanical properties. This study aimed to explore differences in microstructural maturation between the ACL and MCL in postnatal mice to gain insights into their developmental processes. Understanding how normal ACL and MCL tissues develop may help identify key factors that enhance ligament regeneration.

**METHODS:** All animal procedures were approved by the Animal Care Committee at SPU. **Mouse Samples:** ACL and MCL were harvested on postnatal days (P) 4, 14, and 21. **Micro CT:** The hind limbs of 3-week-old mice were prepared and stained with 2.5% phosphotungstic acid (PTA) for five days. Micro-CT ( $\mu$ CT) imaging was performed using a SkyScan system (Bruker), and images were obtained in planes perpendicular to the ACL and MCL using Data Viewer. The cross-sectional areas (CSA) of the ACL and MCL were measured. We calculated the ratio of the CSA of MCL and ACL. **Transmission electron microscopy (TEM):** Ligaments were assessed with TEM for fibril diameter distribution. Ultrathin sections were cut to 75 nm and stained with 0.2% Oolong Tea Extract/PBS for 30 min, followed by lead citrate for 10 min, and photographed. Digital images were acquired using EM1010, JEOL, and Digital Micrograph, Gatan, Inc. **Segmentation and analysis:** The fibrillar regions in the TEM images were identified using Cellpose<sup>2,3</sup>, and the minimum fibril diameter (MFD) and Roundness were measured using ImageJ/Fiji. Roundness was calculated as  $4 \times \text{Area} / [\pi \times (\text{Major axis})^2]$  or as the inverse of the aspect ratio.

**RESULTS SECTION:** Comparing CSA of the ACL and MCL in 3-week-old mice using  $\mu$ CT, the ratio (ACL: MCL) was found to be 70.65: 29.35, indicating that the ACL had a considerably larger CSA (**Figure 1**). TEM Images of the ACL and MCL were shown in **Figure 2A, 2B**. A previous study showed that Achilles tendon fibril diameters were initially small and uniform, as demonstrated at P4. As the mice developed, fibril diameters increased and the distribution of fibril diameter sizes increased significantly larger in the P14 Achilles tendon than in the P4<sup>4</sup>. Given this, this study selected P4 and P14 ligaments. As expected, ACL and MCL at P4 exhibited narrow MFD distributions and sifted to small diameters. By P14, the distributions became broader and shifted toward larger diameters. Comparing the ligaments, the ACL showed a wider distribution and larger MFD values than the MCL at both P4 and P14. These findings indicate that the fibril diameter of the ACL is generally larger than that of the MCL. In the MCL, the roundness values showed a broad distribution at P4, which narrowed at P14 (**Figure 2E**).

**DISCUSSION:** This study investigated the microstructural maturation of the ACL and MCL in postnatal mice. The results showed the ACL exhibited a wider distribution and a large MFD, whereas the MCL showed only a slight widening and an increase. The roundness was plotted for the time series/ligament types in **Figure 2E**. For a perfect circle, roundness = 1. Highly irregular fibril shape (non-circular) means lateral fibril fusion events. The centralization of roundness in the ACL and MCL at each time point did not differ. Roundness slightly decreased throughout the first eight weeks postnatal in mouse tail tendons<sup>5</sup>. These developmental changes may continue for several weeks in both ligaments. In addition,  $\mu$ CT analysis showed that the ACL was larger than the MCL in 3-week-old mice. This suggests that ACL development occurs more prominently than MCL development. CSA and fibril size contribute to ligament mechanical properties. Throughout post-natal development, the mechanical properties, collagen content, mean and standard deviation fibril diameter increased in the Achilles tendon<sup>4</sup>.

Although we didn't measure mechanical properties in this study, these morphological changes may enhance mechanical properties. In conclusion, from a microstructural perspective, this study demonstrates that the development of the ACL, which has a lower intrinsic healing capacity than the MCL, progresses more prominently and at an earlier stage in mice, suggesting that the developmental processes of these two ligaments differ. Further studies revealing molecular differences may contribute to understanding ligament-specific healing mechanisms.

**SIGNIFICANCE/CLINICAL RELEVANCE:** This study demonstrated that the ACL grew faster than the MCL. Early intervention after ACL injury may help enhance its intrinsic healing capacity.

**REFERENCES:** 1. Kokubun+ *AJSM*. 2016; 2. C. Stringer+ *Nat Methods*. 2021; 3. M. Pachitariu+ *bioRxiv* 2025; 4. H. L. Ansgore+ *Ann Biomed Eng* 2011; 5. H. Raymond Hayling+ *Matrix Biol Plus*. 2024.

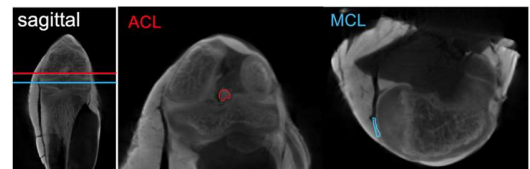


**Figure 1.**  $\mu$ CT images stained with PTA to detect ligament morphology. PTA binds fibrin and collagen solution.

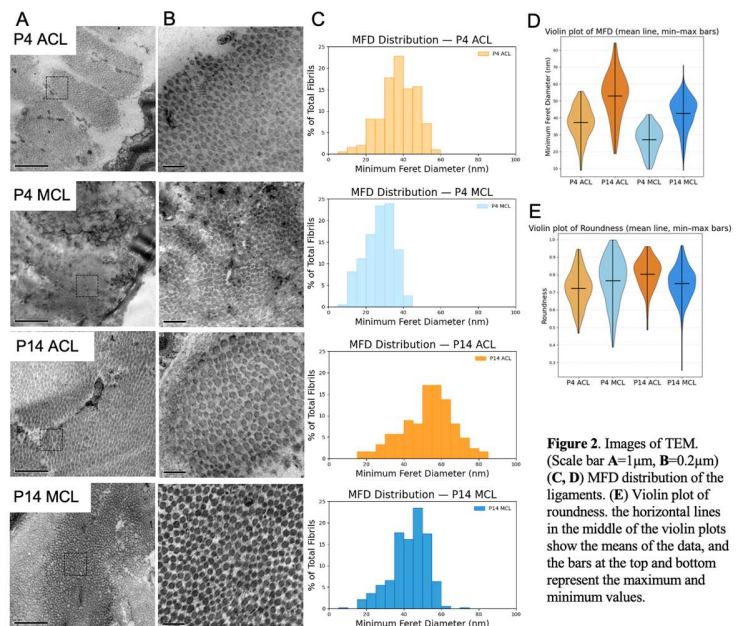


**Figure 2.** Images of TEM. (Scale bar A=1 $\mu$ m, B=0.2 $\mu$ m) (C, D) MFD distribution of the ligaments. (E) Violin plot of roundness, the horizontal lines in the middle of the violin plots show the means of the data, and the bars at the top and bottom represent the maximum and minimum values.